

LQUID-PHASE DISPERSION DURING INJECTION INTO VAPOR-DOMINATED RESERVOIRS

Karsten Pruess

Earth Sciences Division, Lawrence Berkeley Laboratory
University of California, Berkeley, CA 94720

ABSTRACT

The behavior of water injection plumes in vapor-dominated reservoirs is examined. Stressing the similarity to water infiltration in heterogeneous soils, we suggest that ever-present heterogeneities in individual fractures and fracture networks will cause a lateral broadening of descending injection plumes. The process of lateral spreading of liquid phase is viewed in analogy to transverse dispersion in miscible displacement. To account for the postulated "phase dispersion" the conventional two-phase immiscible flow theory is extended by adding a Fickian-type dispersive term.

The validity of the proposed phase dispersion model is explored by means of simulations with detailed resolution of small-scale heterogeneity. We also present an illustrative application to injection into a depleted vapor zone. It is concluded that phase dispersion effects will broaden descending injection plumes, with important consequences for pressure support and potential water breakthrough at neighboring production wells.

INTRODUCTION

Water injection into depleted vapor zones has similarities as well as differences to water injection into unsaturated zones above the water table. In both cases the medium contains a gas (or vapor) phase with very small vertical pressure gradient. Water migrates in response to the combined action of pressure, capillary, and gravity forces. Special effects arise in the geothermal injection problem from the strong coupling between fluid flow and heat transfer, giving rise to boiling and condensation processes and associated two-phase flow effects. Injection of liquid water into vapor-dominated reservoirs generates heat pipe effects (water-vapor counterflow), with very efficient heat transfer (Calore et al., 1986).

In response to liquid injection the water saturation near the injection point will increase. Water saturation may rise all the way to 100 %, establishing single-phase liquid conditions with pressure buildup and consequent lateral flow. If the permeability of the medium is sufficiently high, or water fluxes sufficiently low, the medium will remain in two-phase conditions. Then under isothermal conditions no pressure buildup will occur, and water flow will be affected only by gravity and capillary forces. In media with large pores, such as coarse-grained soils, or "large" fractures in hard rocks, capillary effects tend to be weak, and water flow will be dominated by gravity effects. In this case water will move primarily downward, but "straight" downward flow is only possible when appropriate permeability is available in the vertical direction. Water flowing downward in coarse soils, or in

large (sub-)vertical fractures, may encounter low-permeability obstacles, such as silt or clay lenses in soils, or asperity contacts between fracture walls. Water will pond atop the obstacles and be diverted sideways, until other predominantly vertical pathways are reached (Fig. 1).

When the permeable medium into which water is injected is modeled as homogeneous, with weak capillary effects, injection plumes are predicted to remain narrow and slump essentially vertically downward (Calore et al., 1986; Lai and Bodvarsson, 1991; Shook and Faulder, 1991; Pruess, 1991a). However, horizontal diversion of water from smaller-scale heterogeneities may be an important process. It would tend to broaden injection plumes, with important consequences for heat transfer and vaporization.

The conventional treatment of two-phase flow can model horizontal flow due to pressure and capillary effects. However, horizontal flow diversion from media heterogeneities can be represented only if such heterogeneity is modeled in full explicit detail. In practical applications of reservoir modeling, explicit modeling of small-scale reservoir heterogeneities would require prohibitively large numbers of grid blocks, because heterogeneities occur on many different scales (impermeable lenses, individual fractures, fracture networks, lithologic units, etc.).

It is the purpose of this paper to propose an extension of conventional two-phase flow theory that attempts to capture the essential effects of smaller-scale heterogeneity in an approximate fashion, by adding a dispersive flow term to the governing equations. The validity of the proposed model is examined by means of simulations that represent small-scale heterogeneity in full explicit detail. The paper concludes with illustrative applications to water injection into depleted vapor zones. The simulations were performed with LBL's general-purpose reservoir simulator TOUGH2 (Pruess, 1991b), enhanced with a set of preconditioned conjugate gradient routines to be able to solve problems with of the order of 10,000 grid blocks (G. Moridis, private communication, 1993).

MATHEMATICAL MODEL

The mass balance equation for two-phase single-component flow of water and vapor is customarily written as

$$\frac{\partial}{\partial t} \sum_{\substack{\beta=\text{liquid,} \\ \text{vapor}}} \phi S_{\beta} \rho_{\beta} = -\text{div} \sum_{\substack{\beta=\text{liquid,} \\ \text{vapor}}} \mathbf{F}_{\beta} \quad (1),$$

where ϕ is porosity, S is saturation, ρ is fluid density, and fluid fluxes F_β in liquid and vapor phases are given by a multiphase version of Darcy's law, as follows.

$$F_\beta = -k \frac{k_{r\beta}}{\mu_\beta} \rho_\beta (\nabla P_\beta - \rho_\beta \mathbf{g}) \quad (2).$$

The index β denotes liquid or vapor phase, k is the absolute permeability, $k_{r\beta}$ is relative permeability for phase β , μ is viscosity, P_β is pressure in phase β , and \mathbf{g} is acceleration of gravity. Our proposed Fickian-type diffusion model for phase dispersion involves adding a dispersive flux term for liquid phase to Eq. (2) which, in analogy to solute dispersion in miscible flow (de Marsily, 1986), is written as

$$F_{l,dis} = -\rho_l \phi D_{dis} \nabla S_l \quad (3).$$

We now specialize to conditions where advective flow is dominated by gravity. Introducing the propagation velocity \mathbf{v} of saturation disturbances in the absence of capillary effects (Pruess, 1991a),

$$\mathbf{v} = \frac{k \rho_l \mathbf{g}}{\phi \mu_l} \frac{dk_{rl}}{dS_l} \mathbf{g} \quad (4),$$

the dispersion tensor D_{dis} is written as (Pruess, 1993)

$$D_{dis} = \mathbf{v} \left(\alpha_T [\mathbf{e}_x \mathbf{e}_x + \mathbf{e}_y \mathbf{e}_y] + \alpha_L \mathbf{e}_z \mathbf{e}_z \right) \quad (5).$$

Here we have introduced transverse and longitudinal dispersivities α_T , α_L , and unit vectors \mathbf{e} in the x , y , and z -directions. (Positive z -direction is upward.) \mathbf{g} and \mathbf{v} are the magnitudes, respectively, of the gravitational acceleration and velocity vectors. Inserting Eqs. (4, 5) into (3), the dispersive liquid flux becomes

$$F_{l,dis} = -k \frac{\rho_l \mathbf{g}}{\mu_l} \rho_l \left(\alpha_T [\mathbf{e}_x \mathbf{e}_x + \mathbf{e}_y \mathbf{e}_y] + \alpha_L \mathbf{e}_z \mathbf{e}_z \right) \nabla k_{rl} \quad (6).$$

The flux given by Eq. (6) has been added to Eq. (2), and has been incorporated into our general-purpose reservoir simulator TOUGH2 (Pruess, 1991b). Standard first-order finite difference approximations have been used for discretizing the components of the relative permeability gradient vector.

We note in passing that capillary-driven liquid flux can be written, from Eq. (2), as

$$\begin{aligned} F_{l,cap} &= -k \frac{k_{rl}}{\mu_l} \rho_l \nabla P_{cap} \\ &= -k \frac{\rho_l \mathbf{g}}{\mu_l} \rho_l \left(\frac{1}{\rho_l \mathbf{g}} \frac{dP_{cap}}{d \ln k_{rl}} \right) \nabla k_{rl} \end{aligned} \quad (7).$$

Comparing with Eq. (6), it is seen that the proposed phase-dispersive flux, apart from being anisotropic, has the same structure as capillary flux. The capillary dispersivity is given by

$$\alpha_{cap} = \frac{1}{\rho_l \mathbf{g}} \frac{dP_{cap}}{d \ln k_{rl}} \quad (8).$$

From the correspondence between phase-dispersive and capillary fluxes, we expect that phase dispersion effects may be important when capillary effects are weak, i.e., for liquid flow in "coarse" heterogeneous media such as large fractures and coarse-grained soils. Longitudinal (vertical) phase dispersion will modify the predominant downward advective flow. Transverse dispersion may lead to qualitatively new behavior, causing a lateral (horizontal) spreading of liquid plumes even when capillary pressures are weak. In the remainder of the paper we will focus on transverse dispersion effects.

NUMERICAL EXPERIMENTS

To examine the validity of the proposed phase dispersion model we have performed numerical simulation experiments. In these simulations, small-scale medium heterogeneity was resolved in detail, and no explicit allowance for phase dispersion as in Eq. (6) was made. Liquid plume behavior was explored in media with different types of deterministic and random heterogeneities. As an example, Fig. 2 shows a 2-D vertical section of a medium that features a random distribution of impermeable obstacles. The problem was designed to capture a heterogeneity structure as may be encountered in shallow sedimentary soils (see specifications given in Table 1). Similar parameters may be applicable to individual fractures in vapor-dominated reservoirs. The impermeable obstacles can be interpreted as representing shale, silt, or clay bodies (Begg et al., 1985). In the present context they may be thought of as representing (nearly) impermeable asperity contacts between fracture walls.

TABLE 1. PARAMETERS FOR TEST PROBLEMS WITH DETAILED EXPLICIT HETEROGENEITY.

Permeability	$k = 10^{-11} \text{ m}^2$
Porosity	$\phi = 0.35$
Relative Permeability	
van Genuchten function (1980)	
$k_{rl} = \sqrt{S^*} \left\{ 1 - \left(1 - [S^*]^{1/\lambda} \right)^\lambda \right\}^2$	$S^* = (S_l - S_{lr}) / (1 - S_{lr})$
irreducible water saturation exponent	$S_{lr} = 0.15$ $\lambda = 0.457$
Geometry of Flow Domain	
2-D vertical (X-Z) section	
width (X)	20 m
depth (Z)	15 m
gridding	80 x 120 = 9600 blocks $\Delta X = .25 \text{ m}$ $\Delta Z = .125 \text{ m}$
heterogeneity: random distribution of impermeable obstacles	
Initial Water Saturation	
for $6.5 \leq X \leq 13.5 \text{ m}$ and $-3.5 \leq Z \leq 0 \text{ m}$	$S_l = 0.99$
remainder of domain	$S_l = 0.15$

The numerical experiments involve placing a localized plume of enhanced liquid saturation into a medium such as shown in Fig. 2. The plume is then permitted to flow in

response to gravitational force in isothermal mode, not considering any phase change processes. Plume behavior is analyzed by evaluating spatial moments (Essaid et al., 1993), defined by

$$M_{ijk} = \int x^i y^j z^k \phi (S_1 - S_{10}) dV \quad (9).$$

Plume spreading in the transverse direction is expressed by the mean square plume size, or variance,

$$\sigma_T^2 = \frac{M_{200}}{M_{000}} - \langle x \rangle^2 \quad (10).$$

The center of mass coordinates of the plume are given by

$$\langle x \rangle = M_{100}/M_{000} \quad (11a)$$

$$\langle z \rangle = M_{001}/M_{000} \quad (11b)$$

It is well known that an effective diffusivity for a localized spreading plume can be calculated as (Sahimi et al., 1986; Freyberg, 1986)

$$D_T = \frac{1}{2} \frac{d}{dt} (\sigma_T^2) \quad (12).$$

Dividing by the downward velocity $d\langle z \rangle/dt$ of plume movement yields the transverse dispersivity

$$\alpha_T = \frac{D_T}{(d\langle z \rangle/dt)} \quad (13).$$

Fig. 3 shows transverse dispersivities calculated for two heterogeneous media with different distribution of random obstacles. Initially, dispersivities undergo some transient changes. These are caused by the extreme discontinuity of the initial saturation distribution. For the large initial water saturation of $S_1 = .99$ in the plume water flow rates are large. The consequent rapid saturation changes are poorly resolved with the space and time discretization used in the simulation. As rates of water flow and saturation change slow down the dispersivities are seen to stabilize at very nearly constant values. These results as well as others not shown here confirm that transverse plume spreading from the intrinsic heterogeneities of the medium indeed gives rise to a Fickian diffusion process. We conclude that the heterogeneous medium behaves like an effective dispersive medium.

APPLICATION

To explore and illustrate phase-dispersive effects during water injection into vapor-dominated reservoirs we consider a two-dimensional radially symmetric problem (Fig. 4). An injection well penetrates the top 500 m of a 1000 m thick reservoir. Problem parameters are intended to be representative of conditions in depleted zones at The Geysers (see Table 2; Pruess and Enezy, 1993). The reservoir is described as an effective single-porosity medium, using a large irreducible water saturation of $S_{1r} = 80\%$ to approximate dual-permeability (fracture-matrix) behavior (Pruess, 1983). Initial conditions are a temperature of 240 °C throughout, and gravity-equilibrated pressures relative to 10 bars at the reservoir top. These conditions are maintained at the outer radius of $R = 220$ m, corresponding to an area of approximately 40 acres for the

injection well. Liquid water is injected at a rate of 25 kg/s, and results for water saturation distributions and reservoir pressures after 691.9 days of injection are shown in Figs. 5 and 6.

In the absence of phase dispersion, the injection plume shows a predominant downward movement (Calore et al., 1986; Lai and Bodvarsson, 1991; Shook and Faulder, 1991). Downward as opposed to lateral flow would be even more pronounced for larger permeability, lower injection rate, or coarser discretization with larger cross-sectional area for downward flow of injectate. Gridding in our simulation is fine enough that considerable lateral movement of the injected water takes place. The radius R_g to which the injection plume would have to grow so that water could flow downward under gravity drive at a rate equal to the entire injection rate can be estimated from Eq. (2). For a vertical permeability of $50 \times 10^{-15} \text{ m}^2$ and a rate of 25 kg/s, excluding vaporization effects, we obtain $R_g = 52.1$ m for $T = 240$ °C water, and $R_g = 120.6$ m for $T = 25$ °C water.

Phase dispersion enhances the lateral and diminishes the downward movement of injectate, as expected (Figs. 5b, c). An obvious implication is that neglect of phase-dispersive processes may underestimate the potential for water breakthrough at laterally offset production wells.

TABLE 2. PARAMETERS FOR TWO-DIMENSIONAL R-Z INJECTION PROBLEM.

permeability	$k = 50 \times 10^{-15} \text{ m}^2$
porosity	$\phi = .04$
Rock Properties	
density	$\rho_R = 2600 \text{ kg/m}^3$
specific heat	$c_R = 1000 \text{ J/kg } ^\circ\text{C}$
heat conductivity	$K_R = 2.51 \text{ W/m } ^\circ\text{C}$
Relative Permeability	
Corey-curves	
irreducible water saturation	$S_{1r} = .15$
irreducible gas saturation	$S_{gr} = .05$
Initial Conditions	
temperature	240 °C
pressure	10 bars (at reservoir top)
Injection Specifications	
rate	25 kg/s
enthalpy	$8.4 \times 10^4 \text{ J/kg}$

It is interesting to note that inclusion of phase dispersion diminishes the volume of the single-phase liquid zone and gives rise to very broad two-phase regions. The pressure response from injection shows much detailed spatial structure, with pressures increasing in some regions, decreasing in others (Figs. 6a-c). When phase dispersion is included, more heat transfer and vaporization of injectate are predicted to occur at shallower depths. In the case without phase dispersion most pressure support is coming from the deepest regions. Increasing levels of phase dispersion will confine vaporization and pressure support to shallower depths, but extending to greater distance from the injection well. Pressures near the injection well are considerably lower than in the absence of phase dispersion, especially near the top of the injection interval. These low-pressure regions consume considerable

amounts of vapor by condensation (Pruess and Enezy, 1993). Nearby production wells may respond with flow rate increases or decreases, depending on the elevation difference between open intervals. Production interference will be time-dependent as zones of increased as well as decreased pressures migrate outward from the injector.

DISCUSSION AND CONCLUSIONS

Injection response in vapor-dominated reservoirs is expected to be strongly influenced by heterogeneous reservoir permeability. Even though injected water is likely to flow primarily downward in response to gravitational body force, such flow will be strictly vertical only if appropriate permeability is available. Descending injection plumes will tend to pond atop regions of lower permeability, and will be diverted sideways until again predominantly downward pathways are encountered. Thus, reservoir heterogeneity is expected to cause a lateral broadening of injection plumes.

Stressing the analogy to solute (tracer) dispersion in heterogeneous media, we have proposed a mathematical model that approximates injection plume spreading as a Fickian diffusion process. Support for this concept was provided by simulations with detailed explicit resolution of small-scale permeability heterogeneity. Phase dispersion effects were illustrated by means of an example that is representative of water injection into depleted vapor zones at The Geysers. It was shown that phase dispersion can significantly affect water breakthrough at neighboring production wells. Pressure support through boiling of injectate was predicted to occur below the injection interval, while at shallower depths reservoir steam is consumed by condensation, with associated pressure decline.

It appears that phase dispersion may cause important effects during liquid injection into heterogeneous vapor-dominated reservoirs, and that it should be included in mathematical models. Work is needed to identify appropriate values for phase dispersivities for use in field simulations.

ACKNOWLEDGEMENT

This work was supported by the Assistant Secretary for Energy Efficiency and Renewable Energy, Geothermal Division, of the U.S. Department of Energy under Contract No. DE-AC03-76SF00098. The author thanks his colleague George Moridis for providing a package of preconditioned conjugate gradient routines that made possible the simulation of problems with of the order of 10,000 grid blocks. For a critical review of the manuscript and the suggestion of improvements thanks are due to George Moridis and Marcelo Lippmann.

REFERENCES

- Begg, S.H., D.M. Chang, and H.H. Haldorsen. A Simple Statistical Method for Calculating the Effective Vertical Permeability of a Reservoir Containing Discontinuous Shales, paper SPE-14271, presented at the 60th Annual Technical Conference and Exhibition of the Society of Petroleum Engineers, Las Vegas, NV, September 1985.
- Calore, C., K. Pruess, and R. Celati. Modeling Studies of Cold Water Injection into Fluid-Depleted, Vapor-Dominated Geothermal Reservoirs, Proc., 11th Workshop Geothermal Reservoir Engineering, pp. 161-168, Stanford University, Stanford, California, January 1986.
- de Marsily, G. *Quantitative Hydrogeology*, Academic Press, Orlando, FL, 1986.
- Essaid, H.I., W.N. Herkelrath and K.M. Hess. Simulation of Fluid Distributions Observed at a Crude Oil Spill Site Incorporating Hysteresis, Oil Entrapment, and Spatial Variability of Hydraulic Properties, *Water Resources Res.*, Vol. 29, No. 6, pp. 1753-1770, 1993.
- Freyberg, D.L., A Natural Gradient Experiment on Solute Transport in a Sand Aquifer. 2. Spatial Moments and the Advection and Dispersion of Nonreactive Tracers, *Water Resources Res.*, Vol. 22, No. 13, pp. 2031-2046, 1986.
- Lai, C. H. and G. S. Bodvarsson. Numerical Studies of Cold Water Injection into Vapor-Dominated Geothermal Systems, paper SPE-21788, presented at Society of Petroleum Engineers Western National Meeting, Long Beach, CA, March 1991.
- Pruess, K. Heat Transfer in Fractured Geothermal Reservoirs with Boiling, *Water Resources Res.*, Vol. 19, No. 1, pp. 201-208, 1983.
- Pruess, K. Grid Orientation and Capillary Pressure Effects in the Simulation of Water Injection into Depleted Vapor Zones, *Geothermics*, 20 (5/6), 257-277, 1991a.
- Pruess, K. TOUGH2 - A General Purpose Numerical Simulator for Multiphase Fluid and Heat Flow, Report No. LBL-29400, Lawrence Berkeley Laboratory, Berkeley, CA, May 1991b.
- Pruess, K. Dispersion of Immiscible Fluid Phases in Gravity-Driven Flow: A Fickian Diffusion Model, *Water Resources Res.* (submitted), LBL-33914, June 1993.
- Pruess, K. and S. Enezy. Numerical Modeling of Injection Experiments at The Geysers, Lawrence Berkeley Laboratory Report LBL-33423, presented at 18th Workshop on Geothermal Reservoir Engineering, Stanford University, Stanford, CA, January 26-28, 1993.
- Sahimi, M., B. D. Hughes, L. E. Scriven and H. T. Davis. Dispersion in Flow Through Porous Media - I. One-Phase Flow, *Chem. Eng. Sci.*, 41 (8), 2103-2122, 1986.
- Shook, M. and D. D. Faulder. Analysis of Reinjection Strategies for The Geysers, Proc., Sixteenth Workshop Geothermal Reservoir Engineering, pp. 97-106, Stanford University, Stanford, CA, January 1991.
- van Genuchten, M. Th., A Closed-Form Equation for Predicting the Hydraulic Conductivity of Unsaturated Soils, *Soil Sci. Soc. Am. J.*, Vol. 44, pp. 892-898, 1980.

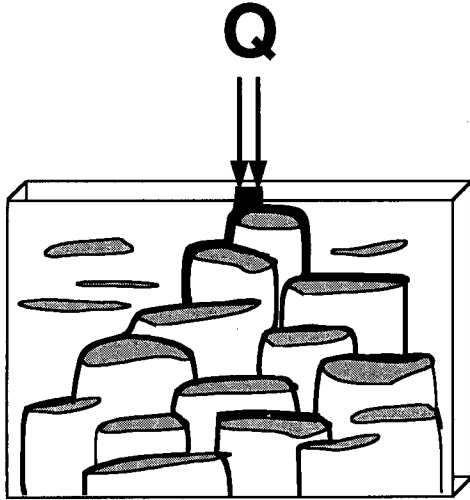


Figure 1. Schematic of water infiltration in a heterogeneous medium. Regions of low permeability (shaded areas) divert water flux sideways and cause a lateral spreading of the infiltration plume.

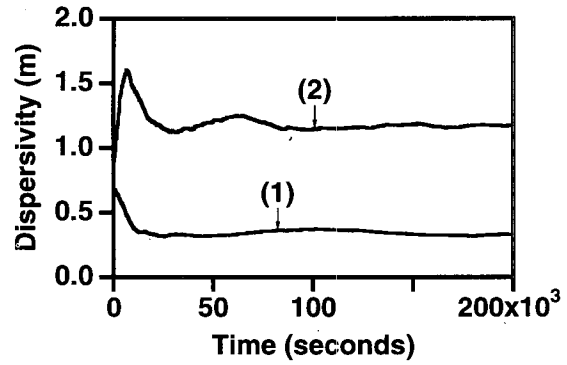


Figure 3. Simulated transverse dispersivities for heterogeneous media with random distributions of 150 impermeable obstacles. Curve (a) is for the medium of Fig. 2; curve (b) is for a medium with length of obstacles uniformly distributed in the range of 1-3 m.

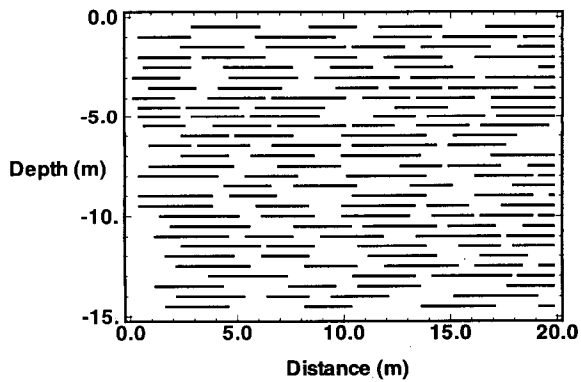


Figure 2. Heterogeneous medium with a random distribution of 150 impermeable obstacles (black segments). Length of obstacles is uniformly distributed in the range of 2-4 m

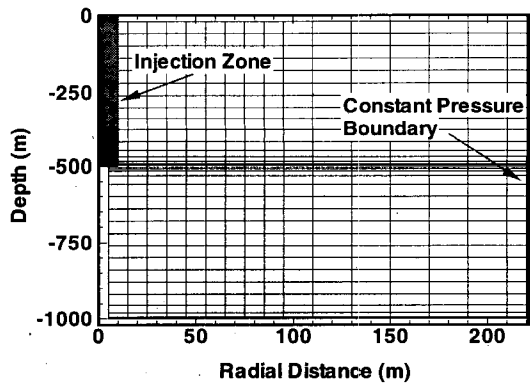
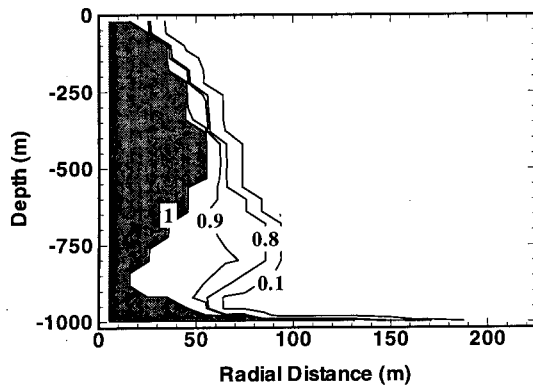
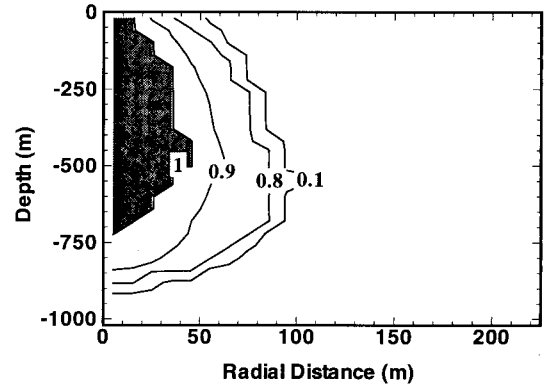


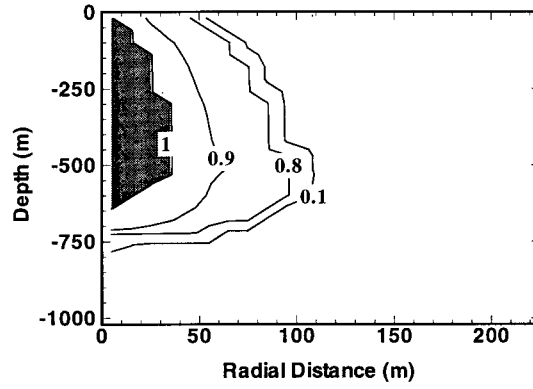
Figure 4. Gridding for two-dimensional R-Z injection problem.



a)

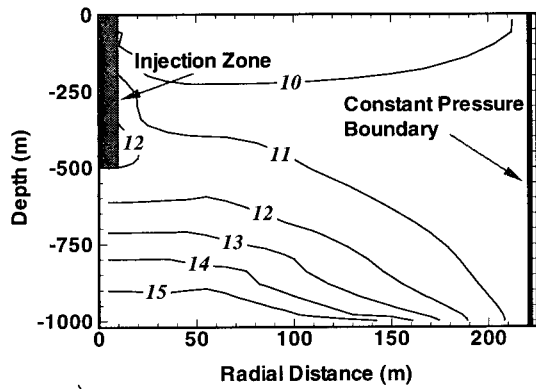


b)

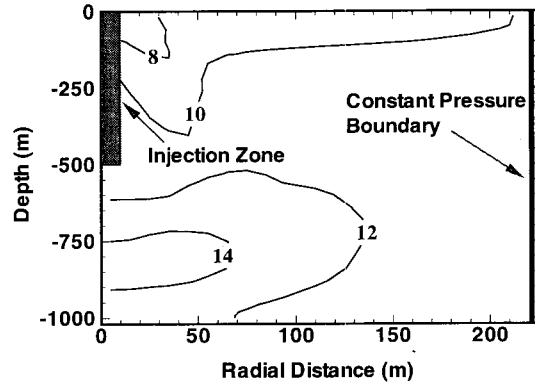


c)

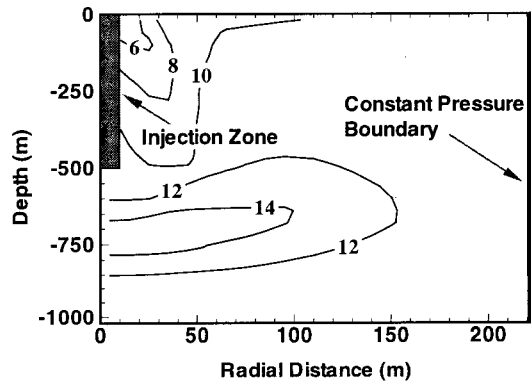
Figure 5. Simulated injection plumes for different transverse dispersivities. Liquid saturation contours after 691.9 days of injection are shown for (a) $\alpha_T = 0$, (b) $\alpha_T = 5$ m, (c) $\alpha_T = 10$ m.



a)



b)



c)

Figure 6. Simulated pressures (in bars) after 691.9 days of injection for phase dispersivities of (a) $\alpha_T = 0$, (b) $\alpha_T = 5$ m, (c) $\alpha_T = 10$ m.